Motion Simulation And Finite Element Analysis Of Knee Prosthesis With Implant

Zhibin Fang[1*], Shaobin Zhang[1], Jiamei Cheng[2], and Shaoming Li[2]

[1] Department of Sports Work, Hebei Agricultural University, Hebei 071000, Hebei, China
[2] College of Science and Technology, Hebei Agricultural University, Huanghua 061100, Hebei, China
[*] Corresponding author. E-mail: 5096026@sohu.com

Received: Feb. 04, 2024; Accepted: Apr. 16, 2024

In this study, we investigated the mechanical behavior of a knee replacement prosthesis (TKR) manufactured by the Zimmer company. To facilitate our analysis, we initially utilized a coordinate measuring device, specifically a contact 3D scanner, to prepare a cloud-of-point model of the prosthesis. This scanning process allowed us to accurately capture the geometry and dimensions of the TKR, providing a detailed representation of its physical structure. By utilizing this advanced scanning technology, we ensured that our subsequent simulations and analyses were based on precise and reliable data, enabling a thorough examination of the mechanical performance of the knee replacement prosthesis. ABAQUS software was then used to analyze the three-dimensional model and nonlinear static analysis was performed on the model. This simulation examined the mechanical performance of the prosthesis for different weight ranges, and the distribution of stress, strain, and displacement within the prosthesis was analyzed. The results show that the maximum stress created in the investigated prosthesis increases from 16MPa to 64MPa per weight of 55 kg to 75 kg. Although, with a 26% increase in the weight of the individual using a knee prosthesis, the maximum stress created in the prosthesis increases by 76%. This type of prosthesis is suitable for the maximum weight category of 80 kg, as it has a reliability coefficient of 3. In light of these results, it is clear that weight categories must be taken into account when considering a particular prosthesis. Otherwise, the prosthesis may be destroyed due to the application of larger forces during various everyday situations and result in serious knee injuries.

Keywords: knee prosthesis, knee joint, finite element analysis, ABAQUS software, stress distribution

http://dx.doi.org/10.6180/jase.202504_28(4).0001

1. Introduction

Among all the joints in the human body, the knee joint is the largest and most complex structurally. Meanwhile, the knee joint has been described as one of the most vulnerable joints in the body due to its large forces, wide range of motion, limited coordination, and reliance on soft tissues. Because of this, knee prostheses have become increasingly popular in recent years to replace damaged joints. In the design of knee prostheses, the main objective is to reconstruct the joint in a manner that enables optimal performance. Accordingly, designers and manufacturers have developed and presented different knee prostheses based on the kinematic behavior and biomechanical characteristics of the knee. Furthermore, much research is being conducted to increase the useful life of prostheses to ensure that patients do not have to undergo repeated surgeries to replace and repair damaged prostheses [1–3].

To analyze the mechanics of the knee joint, researchers use experiments including the study of the knee joint of a corpse and a living organism, as well as numerical and theoretical methods, or mathematical modeling. Due to the geometric complexity of the problem, the complex behavior of the material, the boundary conditions as well as the various loadings in the problem, it is very difficult to reach an exact solution. This problem can be solved by using approximate solutions with an acceptable degree of accuracy within a limited period. A finite element method is one of the best options available in this field [1]. A numerical solution of this kind achieves an approximate solution to many physical and engineering problems whose governing behavior can be expressed by one or more differential equations. Numerous engineering and non-engineering applications have been developed based on the finite element method, including medicine and dentistry. Various artificial body components, such as heart valves, artificial hearts, joint prostheses, dental implants, hearing prostheses, artificial limbs, and hearing implants, have undergone tremendous technological advancements over the years. One of the problems that can be analyzed using the finite element method is the analysis of these artificial components, their functions and connections, and their reaction to body tissues [1].

Estimating the forces and torques acting on the human knee, as well as the torsional forces of the thigh-leg joint, are important factors considered by researchers and designers of prostheses [4–6]. Research using laboratory methods has included the removal of certain constraints, such as ligaments, embedding sensors in several parts of the joints [7], loading of bones and skin, as well as applying force with weights and pulleys instead of muscle force [8–10]. The study examines how joint components are involved in movement control, as well as the effect of injury on the kinematic and kinetic parameters of movement. Even though laboratory studies can provide detailed quantitative information regarding the kinematic and kinetic parameters of movement, these methods are expensive and cannot provide an accurate representation of joint forces during natural movement [1]. Other methods of estimating the force of different components of the knee have included the use of sensitive films to determine contact surfaces and forces, and robotic systems that allow for control of force and movement. It is due to the complexity of applications and the high cost of these devices that they are less widely used. A static and dynamic analysis of knee protrusion prostheses was conducted by De la Mora Ramirez et al. [11]. They examined three different types of prostheses made of titanium alloy, cobalt-chromium alloy, and stainless steel 316L alloy. According to their study, the maximum stress created in these alloys is 47.1, 60.9, and 69.5MPa, respectively, and the maximum compressive stress obtained is 300MPa [11]. To investigate the effect of diseases and injuries, Conlisk et al. [12] examined the model of the injured knee by finite element and compared the results with the model of the healthy knee. In the knee injury model, they simulated meniscus and bone injuries. The results of their study show that meniscus tears in different directions can strongly affect the biomechanics of the knee joint and cause an increase of about 80% in the maximum stress created. Navacchia et al. [13] investigated the effect of minor ligament injuries on knee prosthesis performance. The results of their study show that the damage effect of contact stresses increases in the radial and oblique direction and vice versa due to the increase of the contact surfaces resulting from the rupture, the contact pressure decreases in the longitudinal direction. Kwon et al. [14] analyzed the finite element analysis of the knee replacement prosthesis under the forces and misalignment of the step cycle. After scanning the bone and the knee prosthesis using ANSYS finite element software, they analyzed the nonlinear static analysis of the knee joint and investigated the effect of the prosthesis characteristics on the resulting forces. The results of their study show that the use of suitable prostheses and softer materials causes a compressive stress of about 30MPa in the knee prosthesis. Kang et al. [15] used finite element analysis to analyze the fatigue of knee prostheses with two different genders to investigate the effect of types of materials. They also used the genetic algorithm method to optimize the shape of the prosthesis. The obtained results show the improvement of the shape of the new prosthesis, and the optimal angle has been obtained around 132 degrees. Belvedere et al. [16] designed a new type of knee prosthesis for patients with tumors in the distal femur and proximal tibia regions. Using the finite element method, Li et al. [17] calculated the forces in the ligaments at different angles and under the effect of different forces, as well as the levels and contact stresses in the articular surfaces of the tibiofemoral and patellofemoral joints. Their results show that tearing of the anterior segment ligament causes an increase in the contact stresses in the inner meniscus and the inner surfaces of the joint in the initial angles of flexion, as well as an increase in the force of the lateral ligaments in different angles.

Thienkarochanakul et al. [18] investigated the effects of different loading conditions on the stress distribution within the knee joint. By simulating various activities, such as walking, running, and jumping, the researchers were able to identify the areas of highest stress concentration within the knee joint. This information can be valuable in designing interventions to reduce the risk of knee injuries. In another study by Nikkhoo et al. [19], the researchers focused on the impact of different surgical techniques on the biomechanics of the knee joint. By utilizing FEA, they compared the stress distribution and stability of the knee joint following different surgical procedures, such as total knee replacement and ligament reconstruction. The findings from this study can aid surgeons in making informed decisions regarding the most appropriate surgical technique for individual patients.

The mechanical behavior of knee replacement prostheses plays a crucial role in determining the long-term success and functionality of these devices for patients undergoing knee replacement surgery. Understanding how these prostheses respond to mechanical loading, such as weight-bearing activities and daily movements, is essential for predicting their performance and durability in real-world scenarios. By analyzing the stress, strain, and displacement distribution within knee replacement prostheses, as we have done in our study, clinicians and researchers can gain valuable insights into how these devices withstand varying loads and forces. This knowledge is instrumental in optimizing the design and material selection of knee prostheses to improve their reliability and longevity, ultimately leading to better patient outcomes and reduced risk of complications or implant failure. In summary, the studies conducted in the field of finite element analysis of the knee joint over the past two years have provided valuable insights into the biomechanics, injury mechanisms, and treatment strategies related to this complex joint. By utilizing computational modeling techniques, researchers have been able to simulate various loading conditions, evaluate surgical techniques, and investigate the role of cartilage properties. These findings have the potential to improve clinical decision-making and enhance patient outcomes in the management of knee joint conditions.

The purpose of this research is to investigate the stress distribution on a sample of knee joint replacement prostheses to increase the life of these devices. This allows the effectiveness of a knee prosthesis to be evaluated in a variety of daily activity situations. To mimic the real sample, a titanium alloy GSF knee joint implant (Ti6A14V) with the dimensions and size of the distal femur and proximal tibia will be selected in the current study. In this regard, due to its geometric complexity, a coordinate measuring device, one example of a 3D contact scanner, will be used to model the desired prosthesis by creating high-precision cloud points and editing them with SolidWorks software. The model of the implant will then be created as a 3D model. Simulation of the desired model will be performed using finite element analysis and ABAQUS software as well as nonlinear static analysis. This simulation will investigate the mechanical performance of the implant under various loading conditions and for different weights from 55 kg to 85 kg and in the most critical state. Additionally, the effect of different parameters on the stress distribution and deformation of the implant will be discussed, and a specific weight range for its application will be presented.

2. Materials and methods

In this section, to provide clarity on the steps for creating a geometric model of the knee prosthesis, we outline the methodology supported by the segmentation process with multiple images from various perspectives. Initially, a contact 3D scanner was employed to capture the geometry of the knee prosthesis manufactured by the Zimmer Company. Subsequently, the obtained point cloud data underwent a segmentation process, wherein relevant features of the prosthesis were extracted to create a three-dimensional geometric model. This segmentation process involved delineating the boundaries of individual components of the prosthesis, such as the femoral and tibial components, and refining the geometry to ensure accuracy. To illustrate this process, we present several images from different viewpoints, demonstrating the segmentation of the geometric model and the extraction of key features. These images provide visual support and aid in understanding the methodology employed for creating the geometric model of the knee prosthesis. Fig. 1 depicts a simplified flowchart illustrating the research methodology employed in this study. This flowchart outlines the sequential steps involved in the research process, from capturing the geometry of the knee prosthesis to conducting finite element analysis and interpreting the results. It provides a visual representation of the workflow and procedures followed in the study, enhancing the reproducibility and understanding of the research methodology.

2.1. Creating the geometric model

A three-dimensional geometry of the knee bone is created by first preparing the used knee from CT scan images of a patient's knee and then introducing it as input into Mimics software. An image of the CT scan of the used knee can be seen in Fig. 2. In the following step, Mimix software opens this information and creates a three-dimensional model of the knee. The information is then transformed into a three-dimensional map after modifications are made. As a final step, the raw data was converted into a map for use in finite element analysis using the cloud of point method. In Fig. 3, the geometry of the studied knee is represented in the form of points in the Solidworks software environment.

The purpose of this research has been to examine a real-life example of a knee replacement prosthesis. An illustration of the intended prosthesis can be found in Fig. 4. The knee replacement prosthesis (TKR) is manufactured

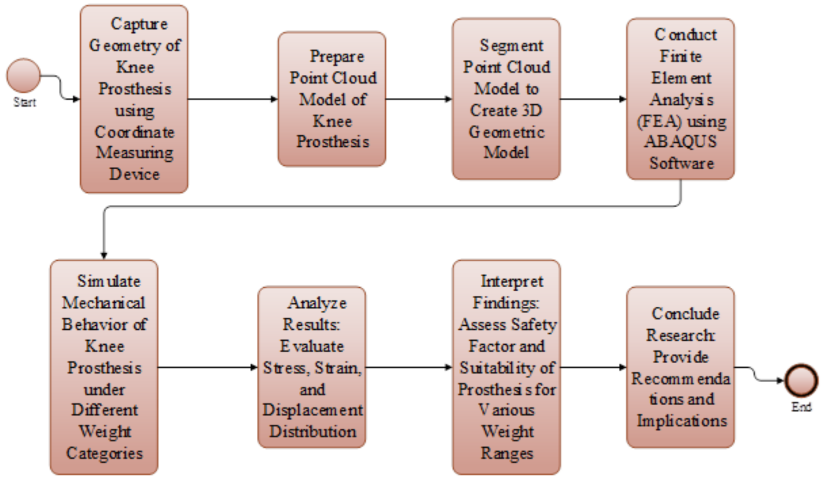

Fig. 1. A simplified flowchart illustrating the research methodology employed in this study

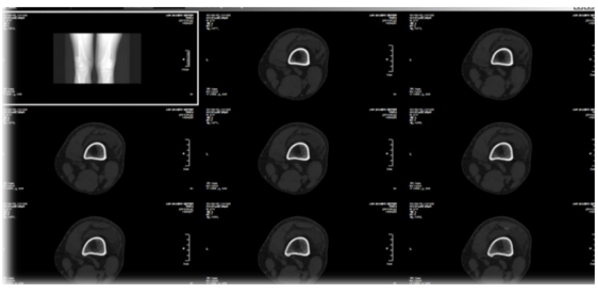

Fig. 2. CT scan images of the used knee

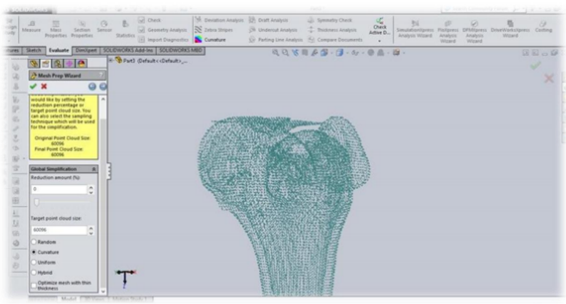

Fig. 3. The studied knee geometry in the Solidworks software environment

by Zimmer and is intended for women. As a result of the geometric complexity of the desired prosthesis, a coordinate measuring device, an example of a contact 3D scanner, is used to prepare the point cloud model of the prosthesis parts.

Fig. 4. The Tibia and femoral parts of the examined knee prosthesis

2.2. Calculation of forces in the knee joint

As shown in Fig. 5, the foot model is defined as a mechanical system consisting of three body parts, the thigh, the leg, and the sole, which are connected two by two to the hip, knee, and ankle joints, respectively.

To determine the forces and torques affecting a joint in a static state, static analysis equations and the free body diagram method are used. It is assumed that the entire body weight is applied to one knee joint in a standing position to draw the free-body diagram of the knee. A depiction of this situation can be found in Fig. 6. Using the distance from the force-extension line from the ground and the vertical force Fy as the body weight, two coplanar forces (Fx and Fz) act on the leg. The external force system acting on the tibia includes three forces that enter the leg from the ground (Fx, Fy, and Fz). Fx is the frictional force on the foot, Fy is the vertical component and Fz is the lateral force from the ground to the foot. In the sagittal plane of the knee, the torque Mz is estimated from the relationship $Mz = Fy \times X$ and $Mz = Fx \times Y$, where X is the vertical distance along Fy and Y is the vertical distance along Fx. X and Y lever arms are calculated from the knee and foot pressure center coordinates. In the coronal plane, the knee torque Mx is

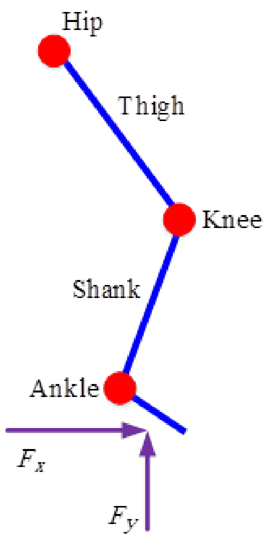

Fig. 5. Free body diagram of the knee joint

calculated from the relations Mx = Fy × Z and Mx = Fz × Y. The forces caused by different weights are calculated analytically for a weight of 60 kg based on Eqs. (1) and (2) and are given in Table 1 for different weights.

$$Fx \times y = Fy \times xFx \times 53 = 588.6 \times 15(\mathrm{y} = 53, \mathrm{x} = 15)Fx = 166.57\ \mathrm{N} \quad (1)$$

$$Fy \times z = Fz \times y588.6 \times 10 = Fz \times 53(\mathrm{z} = 10, \mathrm{y} = 53)Fz = 111.05\ \mathrm{N} \quad (2)$$

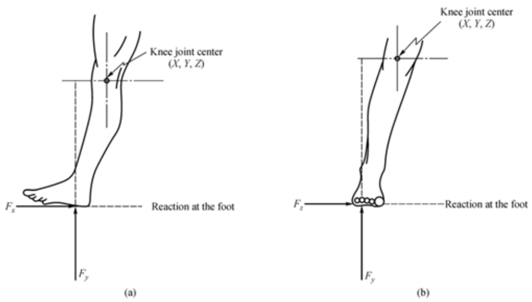

Fig. 6. Free body diagram of the knee joint (a) side view and (b) front view [20]

Table 1. The amount of force on the knee joint for different weights

Weight (kg)	F_x(N)	F_y(N)	F_z(N)
55	152.20	539.89	102.56
60	166.58	588.63	113.54
65	180.46	637.84	126.34
70	194.36	686.34	128.65
75	208.44	735.90	138.45
80	270.23	895.32	153.23

2.3. Finite element simulation

The use of the finite element method has been developed in many different fields of engineering sciences such as civil engineering, mechanics, and biomechanics [21–25]. The assumptions of the simulation problem will be presented first in this section. Subsequently, owing to its geometric complexity, the desired prosthesis will be modeled using a coordinate measuring device. An example of a three-dimensional contact scanner will be employed to create a cloud of precise points, which can be edited with Solid-Works commercial software. A finite element numerical method will be used to simulate the prepared model using ABAQUS commercial software. Various weight categories will be analyzed to evaluate the stress-strain on the knee prosthesis during critical daily activities.

A 3D model of the different parts of the prosthesis is prepared and edited to enable numerical simulation using the ABAQUS software. Initially, a point cloud model is created by scanning the knee prosthesis using a coordinate measuring device. Subsequently, the resulting point cloud model undergoes editing to convert it into a 3D model suitable for simulation purposes. This editing process involves refining the geometry, smoothing surfaces, and ensuring the model's compatibility with the finite element analysis techniques employed in ABAQUS software. The edited 3D model accurately represents the geometry and features of the knee prosthesis, facilitating precise simulation of its mechanical behavior under various loading conditions. To this end, a 3D model of a prosthetic part was created and modified using SolidWorks commercial software. As part of the editing process of the prosthetic parts, an attempt has been made to remove the sharp edges. Also, at the contact points and other points that caused fine meshes, the surfaces were stitched together and unnecessary parts were removed for analysis. Fig. 7illustrates the 3D model of different components of a prosthetic device.

In this study, a non-linear static analysis will be conducted using the finite element method and the commercial software ABAQUS for simulating the knee prosthesis in question with enriched molecular polyethylene. The

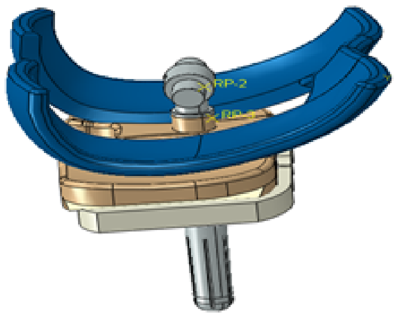

Fig. 7. 3D model of the femoral part of the knee prosthesis of the case

specifications of the materials employed in human knee replacement prostheses are presented in Tables 2 and 3. Table 2 provides the elastic characteristics of the material used, while Table 3 presents the plastic stress-strain properties of the material employed in the femoral, femur, and tibia parts. These tables will serve as references for defining the material properties within the finite element model, ensuring an accurate representation of the mechanical behavior of the knee prosthesis under varying loading conditions.

Due to the geometrical complexity of knee prosthesis members, the assembly was meshed in ABAQUS using 10-node tetrahedral elements (C3D10), with a seed size of 1.5 mm to ensure adequate mesh density. Mesh convergence was assessed to verify the sensitivity of the results to changes in the mesh density. An ABAQUS-based mesh verification method was employed to ensure that the percentage of element distortion for all models remained below 0.22%. This rigorous verification process helps to ensure the accuracy and reliability of the finite element analysis results obtained using the meshed models. Also, in Fig. 8, the forces and range of different movements applied to the femoral and leg parts of the prosthesis are shown. In the knee prosthesis, the degrees of freedom in the lateral directions are restricted $(U1 = U2 = 0)$, and the end of the tibia bone is completely restricted $(U1 = U2 = U3 = 0)$. In addition, to model the contact between different components, the contact adverb has been used. After modeling and applying loading and contact and boundary constraints and solving using the finite element method, it is possible to observe the stresses applied to each part of the different members and compare it with different criteria to the optimal design of the members by considering and changing Thickness, material, etc.

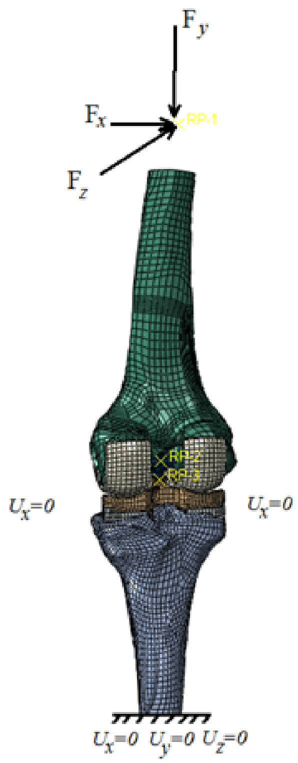

Fig. 8. The meshed model of the knee and prosthesis assembly along with the representation of the forces and boundary conditions of the knee members

3. Results

In this section, the results of the knee prosthesis simulation using the finite element method via ABQUS software are presented along with different force conditions for different weight categories.

3.1. Mesh independency study

This part examines the lack of dependence on the simulation mesh of the desired knee prosthesis. According to Table 4, when the element is increased several times, the von Mises stress changes slightly. In other words, the von Mises stress parameter does not depend on the number of elements, indicating its convergence. During this study, 689154 elements and 985456 nodes were used, which predicted a von Mises equivalent stress of 16.66 MPa with a deviation of 0.4% from the converged stress with 597486 elements.

3.2. Stress distribution

In the initial analysis, simulation results for the 55 kg weight category are presented, focusing on the equivalent

Table 2. Characteristics of knee replacement prosthesis materials

	Material	Poison ratio	Young Modulus	Density
Femoral	Ti-6Al-4V	0.32	116GPa	4620 kg m^{-3}
Tibia	UHMWPE	0.44	1.1GPa	920 kg m^{-3}
Femur	Bone	0.45	10.5MPa	1550 kg m^{-3}

Table 3. Stress-plastic strain of materials used in knee prosthesis

Strain	Stress (MPa)
0	14
0.0367	15.73
0.0472	18.35
0.2834	30.42
0.3465	33.00

Table 4. Investigation of independence from the mesh for knee prosthesis

Solution Number	Mesh Size (mm)	Elements	Equivalent Stress (MPa)	Change (%)
1	10	39478	4.23	-
2	8	78921	7.84	45.8
3	6	178568	12.17	35.0
4	3	220468	14.92	20.0
5	2	426820	16.02	6.3
6	1	597427	16.52	3.1
7	0.5	682590	16.63	0.4

stress distribution. Fig. 9 depicts the von Mises stress contour of various components, including the prosthetic parts, femur bone, and tibia bone, under the application of forces resulting from a 55 kg weight load. It is observed that the maximum stress values in the femur, tibia, and knee prosthesis are 0.15MPa, 0.97MPa, and 16.60MPa, respectively. Notably, the stress concentration is higher in the knee prosthesis due to the presence of contact areas. However, it is reassuring that the maximum stress in the prosthesis remains below the yield stress of titanium. Consequently, the prosthesis exhibits an acceptable safety margin in this weight category, with a calculated safety factor of approximately 54 . This analysis underscores the mechanical robustness of the prosthesis under typical loading conditions for individuals weighing 55 kg, affirming its suitability for clinical use in this demographic group.

Fig. 10 illustrates the von Mises stress contour of the prosthetic parts, femur bone, and tibia bone for a weight of 60 kg. In this scenario, the von Mises stress values for the femur, tibia, and knee prosthesis are recorded as 0.53MPa, 1.03MPa, and 45.68MPa, respectively. It is evident from the finite element analysis results that the stress experienced by the knee prosthesis is significantly higher in this case. However, despite the elevated stress levels, the material properties of the prosthesis ensure that it operates within a safe range and remains sufficiently distant from the plastic deformation zone. With respect to the yield stress of the prosthesis material, the calculated safety factor for this weight category stands at 23. This analysis underscores the resilience of the prosthesis design, indicating its ability to withstand increased mechanical loads associated with individuals weighing 60 kg while maintaining structural integrity and safety.

Considering the weight category of 65 kg, the results of the simulation including the equivalent stress of the prosthesis parts, femur bone and tibia bone are shown in Fig. 11. The results of the finite element analysis show that for a weight of 65 kg, the maximum von Mises stress generated in the femur, tibia and prosthesis is 0.91MPa, 1.10MPa and 56.26MPa, respectively. In this case, the safety factor of the knee prosthesis is equal to 16 .

Fig. 12 shows the von Mises stress contour of prosthetic parts, femur bone and tibia bone by applying the forces resulting from the weight of 75 kg. According to the finite element results presented in this figure, it can be seen that the maximum von Mises stress generated in the femur bone, tibia bone, and knee prosthesis is 1.61MPa, 1.26MPa, and 75.72MPa, respectively. As the results show, in this case, the stress created in the prosthesis is much higher, but due to the material used in the prosthesis, the prosthesis still operates in a safe area and is far enough away from the plastic area. Because the surface of the knee prosthesis has more contact surface, therefore, support pressure and more stress are created in this part. According to the yield

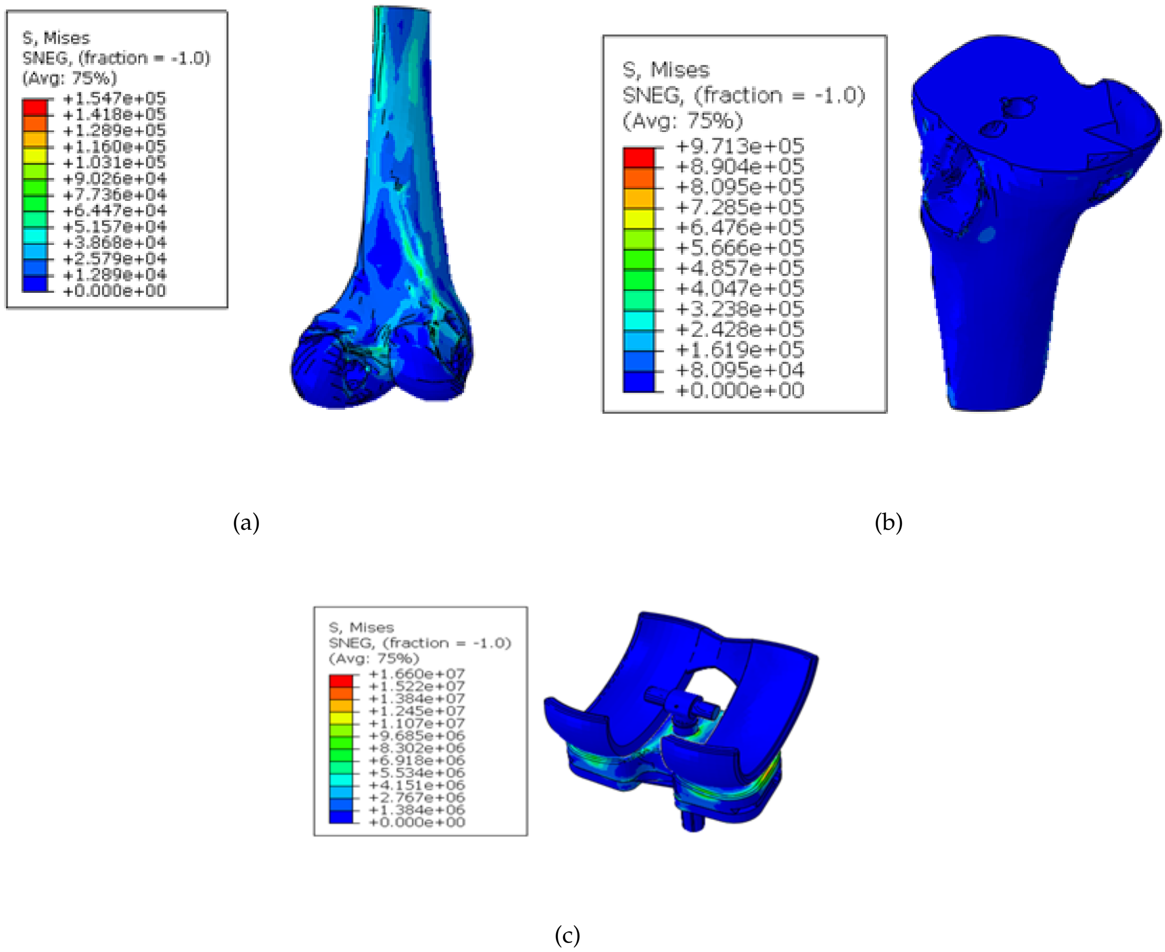

Fig. 9. Stress distribution (Pa) in (a) femur, (b) tibia and (c) knee prosthesis for 55 kg weight

stress of the prosthesis, the safety factor of the prosthesis is 11.8 in this weight category. Considering that the reliability factor, in this case, was extracted for static analysis and its value is somewhat lower, therefore, considering dynamic analysis or sudden application of force to the knee, the prosthesis may enter the plastic area. And a lasting change in its shape.

Based on this, it can be stated that considering the margin of confidence, the ability to use this type of knee prosthesis is not suitable for weight categories greater than 75 kg. In addition, it is observed that the stress of the tibia bone is about 14% more than that of the femur bone.

In this section, simulation results depicting the equivalent stress distribution in the prosthetic parts, femur bone, and tibia bone for the 85 kg weight category are presented in Fig. 13. The finite element analysis reveals that for a weight of 85 kg, the maximum von Mises stress observed in the knee prosthesis reaches 912MPa. These findings indicate that the safety factor for the knee prosthesis falls below 1 , suggesting that the prosthesis is unable to withstand weights exceeding the specified weight category of 80 kg. Consequently, it is evident that this particular prosthesis design may not be suitable for individuals weighing 85 kg or more due to the risk of structural failure under applied loads. This analysis underscores the importance of considering weight categories in prosthesis selection to ensure patient safety and avoid potential complications associated with mechanical overloading of the implant.

3.3. Comparison of results between different weight categories

Based on the finite element analysis conducted in the previous sections, this section compares the maximum von Mises stress generated in different parts of the knee, as well as the reliability coefficient of the knee prosthesis. A

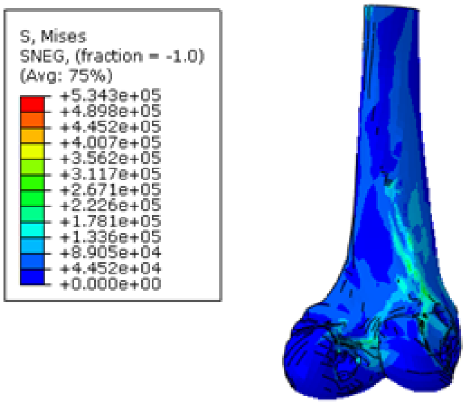

(a)

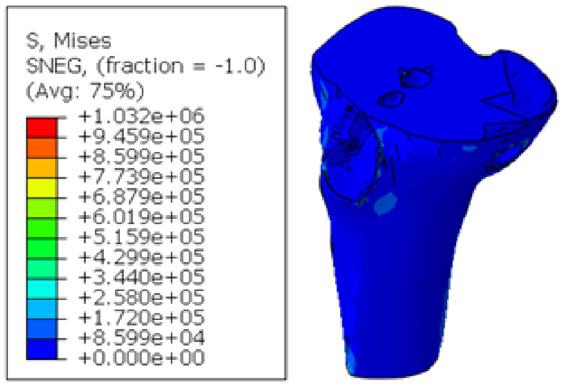

(b)

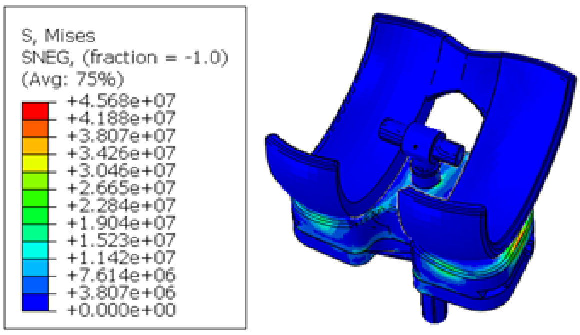

(c)

Fig. 10. Stress distribution (Pa) in (a) femur, (b) tibia, and (c) knee prosthesis for 60 kg weight

summary of the results of the finite element analysis can be found in Table 5. Examining these results, it is apparent that the tibia bone is subjected to more stress than the femur bone and that the knee prosthesis is subjected to the greatest amount of stress. Moreover, by examining the confidence factor created in the knee prosthesis under various weight categories, it is evident that the knee prosthesis has a safety factor of about 15 at a weight of 75 kg. Considering the confidence margin, it can be concluded that this weight category is appropriate for the prosthesis under investigation.

The limitation of using von Mises stress in examining stress distribution in bones lies in its applicability to materials with homogeneous and isotropic properties. Bones, however, exhibit complex material properties, including anisotropy, viscoelasticity, and heterogeneity. Additionally, bone response to loading varies with factors such as loading rate, direction, and the presence of microstructural features like trabecular and cortical bone. Von Mises stress analysis assumes uniform stress distribution and may oversimplify the complex stress patterns present in bones. Therefore, while von Mises stress can provide useful insights, particularly in ductile materials, its application to bone biomechanics requires careful consideration of these limitations. Integrating other analysis techniques and considering bone-specific characteristics can enhance the ac-

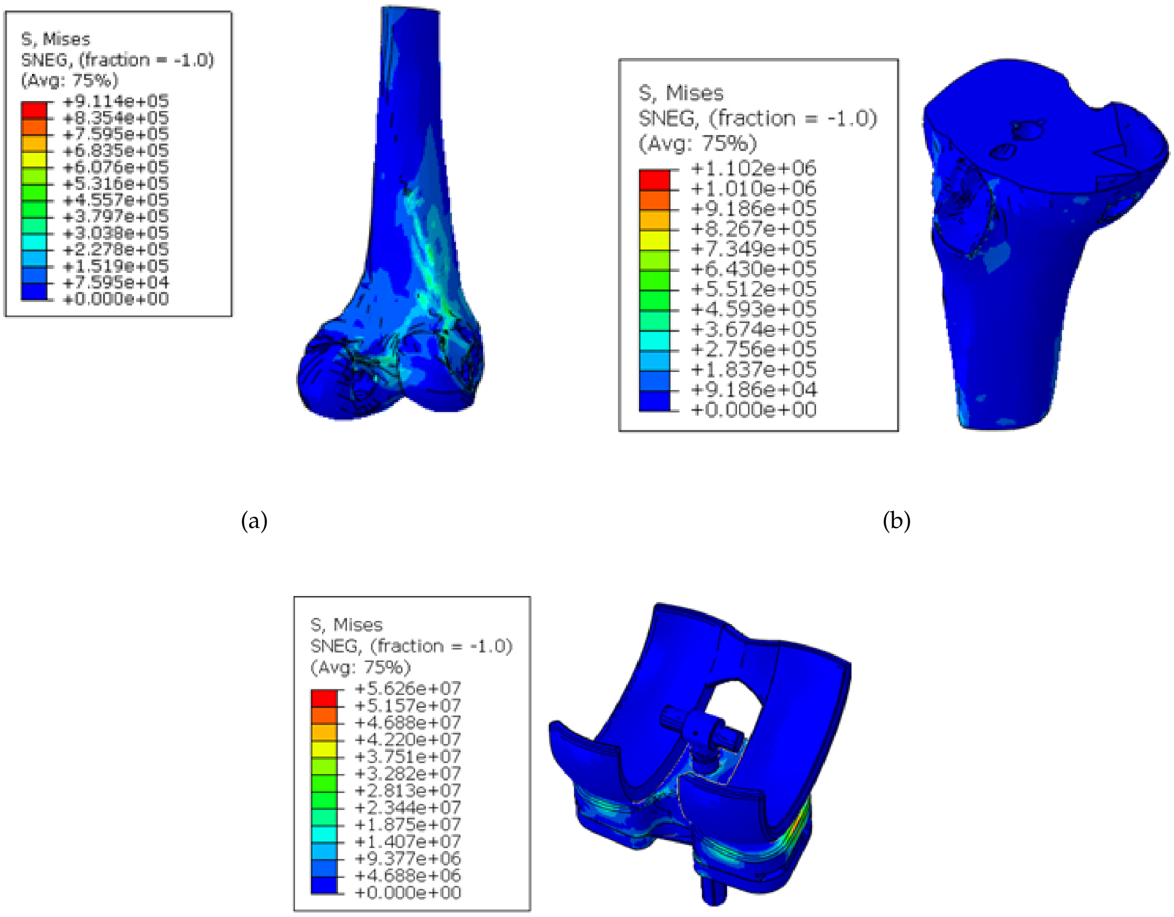

(a) (b)

(c)

Fig. 11. Stress distribution (Pa) in (a) femur, (b) tibia and (c) knee prosthesis for 65 kg weight

Table 5. Maximum von Mises stress created in the femur bone, tibia bone and knee prosthesis for different weight categories

Weight	Femur (MPa)	Tibia (MPa)	Prosthesis (MPa)	Safety Factor
55 kg	0.15	0.97	16.60	62.23
60 kg	0.53	1.03	45.68	22.63
65 kg	0.91	1.10	56.26	17.45
70 kg	1.22	1.24	63.32	16.75
75 kg	1.61	1.26	75.72	14.73
80 kg	2.24	3.22	277.04	3.12
85 kg	3.45	4.23	912.0	0.98

curacy and reliability of stress distribution assessments in bones. Potential limitations of the study include the simplifications inherent in the finite element model used, which may not fully capture the complexity of knee prostheses or surrounding tissues. Additionally, the chosen material properties and boundary conditions might not entirely represent real-world scenarios, impacting the accuracy of the results. Further validation against experimental data or clinical outcomes could strengthen the findings, as could exploring patient-specific modeling approaches. Avenues for future research encompass biomechanical optimization of prosthetic designs and materials, longitudinal studies on long-term outcomes, integration of multiscale modeling techniques, and exploration of advanced simulation

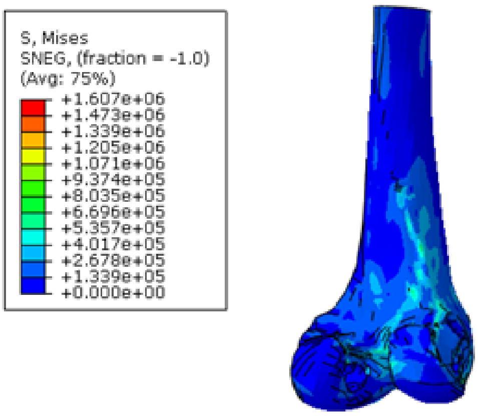

(a)

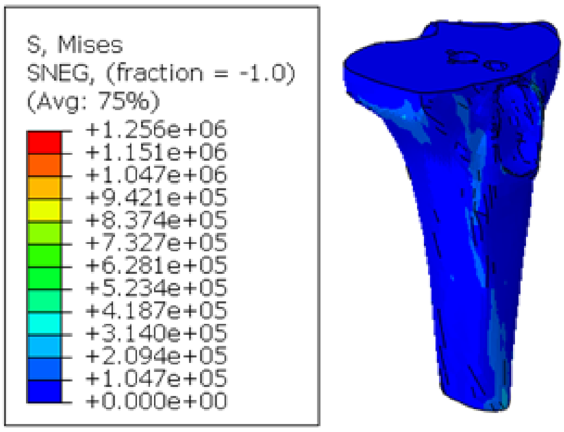

(b)

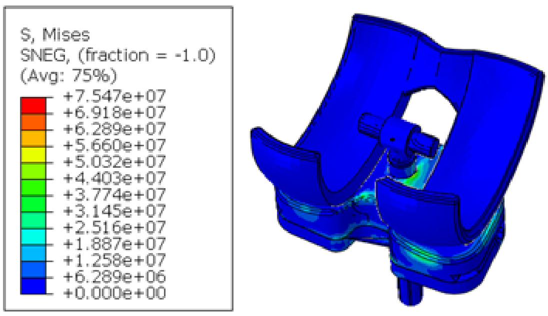

(c)

Fig. 12. Stress distribution (Pa) in (a) femur, (b) tibia and (c) knee prosthesis for 75 kg weight

methods to better understand knee prosthetic behavior and improve patient outcomes.

4. Conclusion

In this research, the mechanical behavior of a real sample of knee replacement prosthesis (TKR) for women manufactured by Zimmer Company has been investigated. As a result of its geometric complexity, the desired prosthesis was modeled using a coordinate measuring device, which is an example of a contact 3D scanner, in order to create cloud points with high accuracy. Using SolidWorks software, the model is modified and then simulated with ABAQUS commercial software and analyzed via finite element numerical methods. The stress-strain of the knee prosthesis was evaluated for the range of 50 kg to 85 kg. The following conclusions were reached based on the results:

- For weights of 55 kg to 75 kg, the maximum von Mises stress created in the femur bone changes from 0.15MPa to 1.61MPa, for the tibia bone from 0.16MPa to 3.22MPa, and for the knee prosthesis from 16.55MPa to 75.72MPa.
- For a weight of 70 kg, the maximum von Mises stress in the femur bone, tibia bone, and knee prosthesis is 1.22MPa, 1.24MPa, and 63.39MPa, respectively. Based on these results, it can be seen that the stress created in the tibia bone is about 25.6% more than the femur bone and the confidence factor for knee prosthesis is about 14.05.
- For different weights in fixed positions, the used prosthesis can bear up to 75 kg in weight categories. At a weight of 75 kg, the safety factor of the knee prosthesis is about 12, so the use of this type of prosthesis is not

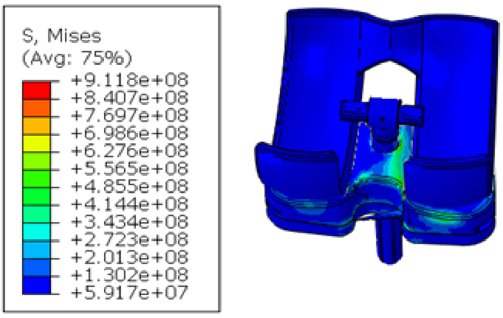

Fig. 13. Distribution of knee prosthesis stress per weight of 85 kg

recommended for people weighing more than 75 kg. The results show that the safety factor of the analyzed prosthesis for a weight of 80 kg is around 3 , which is a very small value. It can also be seen that for the weight category of 85 kg, the safety coefficient was less than unity, so this prosthesis will not be able to be used for weight categories greater than 80 kg.

In conclusion, this study underscores the critical importance of considering weight categories in the selection of knee replacement prostheses to optimize mechanical performance and enhance patient outcomes. To address this, we offer practical recommendations for clinicians and prosthetists: Firstly, clinicians should factor in patient weight categories when selecting knee prostheses to minimize the risk of implant failure, particularly for individuals with higher body mass indices. Secondly, prosthetists are encouraged to explore avenues for optimizing prosthesis design, potentially through innovative modifications or materials, to improve durability and functionality across different weight ranges. By integrating these recommendations into clinical practice, healthcare professionals can make more informed decisions regarding prosthesis selection and design, thereby contributing to improved patient satisfaction and long-term success following knee replacement surgery.

Funding

This study was supported by the Project of the Liaoning Provincial Department of Science and Technology [Research on Building ES-DSA Model to Improve Energy Thermal Efficiency of Dalian Hongyanhe Nuclear Power Plant].

References

[1] S. Kumar and S. Bhowmik, (2022) *"Potential use of natural fiber-reinforced polymer biocomposites in knee prostheses: A review on fair inclusion in amputees"* **Iranian Polymer Journal *31***: 1297–1319.

[2] Y. Sun, H. Tang, Y. Tang, J. Zheng, D. Dong, X. Chen, F. Liu, L. Bai, W. Ge, and L. Xin, (2021) *"Review of recent progress in robotic knee prosthesis related techniques: Structure, actuation and control"* **Journal of Bionic Engineering *18***: 764–785.

[3] R. Fluit, E. C. Prinsen, S. Wang, and H. V. D. Kooij, (2019) *"A comparison of control strategies in commercial and research knee prostheses"* **IEEE transactions on biomedical engineering *67***: 277–290.

[4] V. Kanaujia, A. Gupta, D. K. Sharma, S. Verma, and R. K. Yadav, (2020) *"Study of effectiveness of lateral wedge insole on medial compartment of osteoarthritis of knee treated with viscosupplementation"* **Indian Journal of Pain *34***: 106–111.

[5] E. Esfandiari, M. A. Sanjari, A. A. Jamshidi, M. Kamyab, and H. R. Yazdi, (2020) *"Gait initiation and lateral wedge insole for individuals with early knee osteoarthritis"* **Clinical Biomechanics *80***: 105163.

[6] M. Mannisi, A. Dell'Isola, M. S. Andersen, and J. Woodburn, (2019) *"Effect of lateral wedged insoles on the knee internal contact forces in medial knee osteoarthritis"* **Gait & posture *68***: 443–448.

[7] K. A. Marriott and T. B. Birmingham, (2023) *"Fundamentals of Osteoarthritis. Rehabilitation: exercise, diet, biomechanics, and physical therapist-delivered interventions"* **Osteoarthritis and Cartilage**:

[8] L. Shu, N. Abe, S. Li, and N. Sugita, (2022) *"Importance of posterior tibial slope in joint kinematics with an anterior cruciate ligament-deficient knee"* **Bone & Joint Research *11***: 739–750.

[9] A. Grassi, G. D. Fabbro, S. D. Paolo, F. Stefanelli, L. Macchiarola, G. A. Lucidi, and S. Zaffagnini, (2019) *"Medial and lateral meniscus have a different role in kinematics of the ACL-deficient knee: a systematic review"* **Journal of ISAKOS *4***: 233–241.

[10] D. Wang, R. N. K. III, M. J. Amirtharaj, B. M. Hardy, D. H. Nawabi, T. L. Wickiewicz, A. D. Pearle, and C. W. Imhauser, (2019) *"Tibiofemoral kinematics during compressive loading of the ACL-intact and ACL-sectioned knee: roles of tibial slope, medial eminence volume, and anterior laxity"* **JBJS *101***: 1085–1092.

[11] T. De la Mora Ramirez, M. Doñu Ruiz, I. Hilerio Cruz, N. López Perrusquia, and E. García Bustos, (2019) *"Topological and Contact Force Analysis of a Knee Tumor Prosthesis"* **Engineering Design Applications**: 291–304.

[12] N. Conlisk, C. R. Howie, and P. Pankaj, (2016) *"An efficient method to capture the impact of total knee replacement on a variety of simulated patient types: A finite element study"* **Medical Engineering & Physics *38***: 959–968.

[13] A. Navacchia, P. J. Rullkoetter, P. Schütz, R. B. List, C. K. Fitzpatrick, and K. B. Shelburne, (2016) *"Subject-specific modeling of muscle force and knee contact in total knee arthroplasty"* **Journal of Orthopaedic Research *34***: 1576–1587.

[14] O.-R. Kwon, K.-T. Kang, J. Son, D.-S. Suh, C. Baek, and Y.-G. Koh, (2017) *"Importance of joint line preservation in unicompartmental knee arthroplasty: finite element analysis"* **Journal of Orthopaedic Research *35***: 347–352.

[15] K.-T. Kang, J. Son, O.-R. Kwon, and Y.-G. Koh, (2017) *"Malpositioning of prosthesis: patient-specific total knee arthroplasty versus standard off-the-shelf total knee arthroplasty"* **JAAOS Global Research & Reviews *1***: e020.

[16] C. Belvedere, A. Leardini, F. Catani, S. Pianigiani, and B. Innocenti, (2017) *"In vivo kinematics of knee replacement during daily living activities: condylar and post-cam contact assessment by three-dimensional fluoroscopy and finite element analyses"* **Journal of orthopaedic research *35***: 1396–1403.

[17] L. Li, L. Yang, K. Zhang, L. Zhu, X. Wang, and Q. Jiang, (2020) *"Three-dimensional finite-element analysis of aggravating medial meniscus tears on knee osteoarthritis"* **Journal of orthopaedic translation *20***: 47–55.

[18] K. Thienkarochanakul, A. A. Javadi, M. Akrami, J. R. Charnley, and A. Benattayallah, (2020) *"Stress distribution of the tibiofemoral joint in a healthy versus osteoarthritis knee model using image-based three-dimensional finite element analysis"* **Journal of Medical and Biological Engineering *40***: 409–418.

[19] M. Nikkhoo, K. Hassani, A. T. Golpaygani, and A. Karimi, (2020) *"Biomechanical role of posterior cruciate ligament in total knee arthroplasty: a finite element analysis"* **Computer Methods and Programs in Biomedicine *183***: 105109.

[20] M. A. Kumbhalkar, U. Nawghare, R. Ghode, Y. Deshmukh, and B. Armarkar, (2013) *"Modeling and finite element analysis of knee prosthesis with and without implant"* **Universal Journal of Computational Mathematics *1***: 56–66.

[21] J. Esmaeili, K. Andalibi, O. Gencel, F. K. Maleki, and V. A. Maleki, (2021) *"Pull-out and bond-slip performance of steel fibers with various ends shapes embedded in polymer-modified concrete"* **Construction and Building Materials *271***: 121531.

[22] E. Altas, F. Khosravi, H. Gokkaya, V. A. Maleki, Y. Akınay, O. Ozdemir, O. Bayraktar, and H. Kandas, (2022) *"Finite element simulation and experimental investigation on the effect of temperature on pseudoelastic behavior of perforated Ni–Ti shape memory alloy strips"* **Smart Materials and Structures *31***: 025031.

[23] M. H. Alizadeh, M. Ajri, and V. A. Maleki, (2023) *"Mechanical properties prediction of ductile iron with spherical graphite using multi-scale finite element model"* **Physica Scripta *98***: 125270.

[24] J. Esmaeili, K. Andalibi, and O. Gencel, (2021) *"Mechanical characteristics of experimental multi-scale steel fiber reinforced polymer concrete and optimization by Taguchi methods"* **Construction and Building Materials *313***: 125500.

[25] J. Esmaeili and K. Andalibi, (2019) *"Development of 3D Meso-Scale finite element model to study the mechanical behavior of steel microfiber-reinforced polymer concrete"* **Computers and Concrete, An International Journal *24***: 413–422.